Supplement of Atmos. Chem. Phys., 20, 6921–6951, 2020
https://doi.org/10.5194/acp-20-6921-2020-supplement

Atmospheric Chemistry and Physics
Open Access

Supplement of

Marine organic matter in the remote environment of the Cape Verde islands – an introduction and overview to the MarParCloud campaign

Manuela van Pinxteren et al.

Correspondence to: Manuela van Pinxteren (manuela@tropos.de) and Hartmut Herrmann (herrmann@tropos.de)

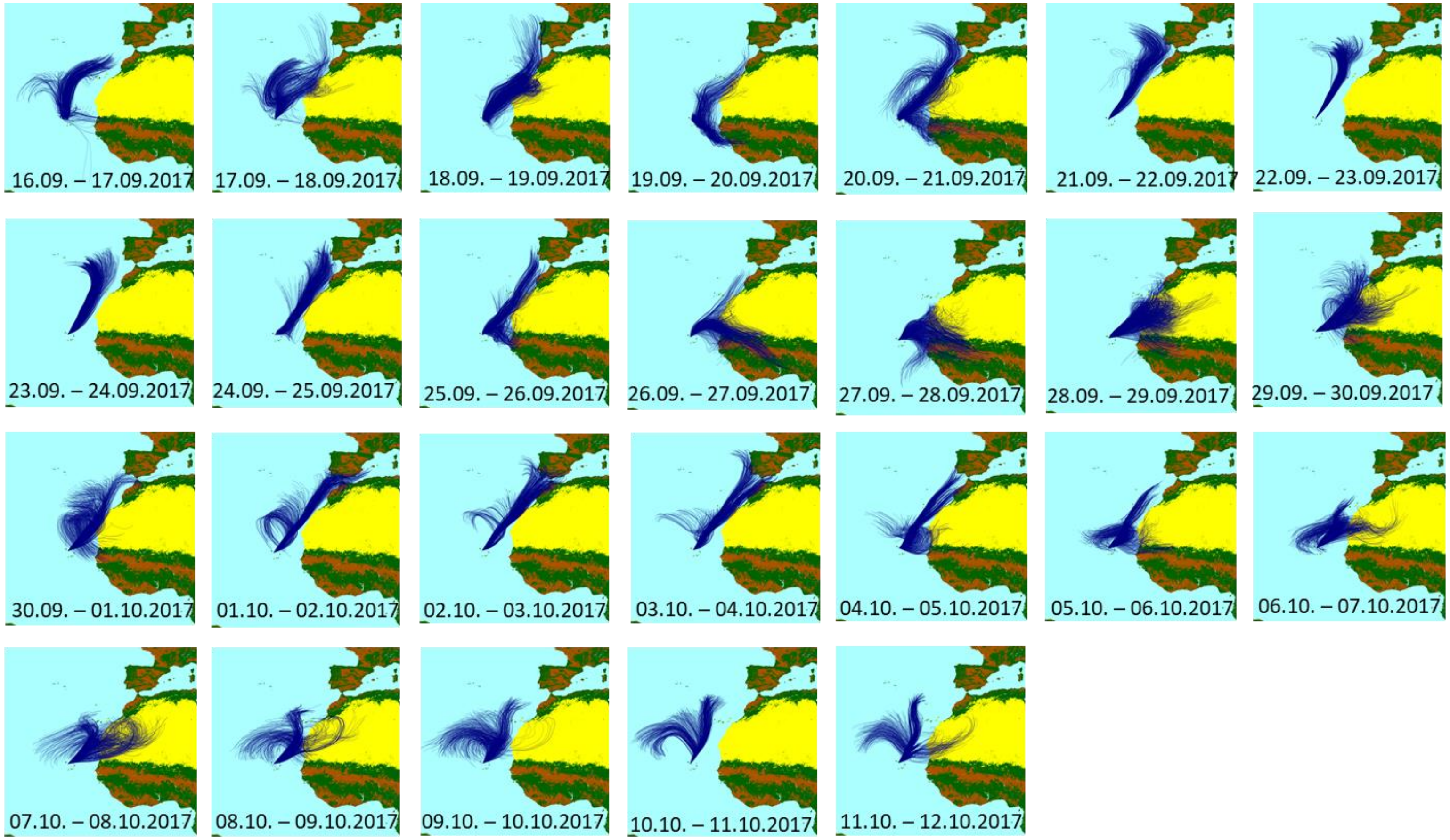

Fig. S1: *96 hour back trajectories calculated on an hourly basis within the intervals of the aerosol particle filter sampling at the CVAO, using the NOAA HYSPLIT model (HYbrid Single-Particle Lagrangian Integrated Trajectory, http://www.arl.noaa.gov/ready/hysplit4.html, 26.07.19) in the ensemble mode at an arrival height of 500 m ± 200 m ((van Pinxteren, et al. 2010)).Starting time of the trajectories corresponded with the sampling time of the aerosol particles and was 21.00 UTC from 16th – 21st September and 16.00 UTC from 22nd September – 12th October.*

Helikite

The measurements were done next to the CVAO using a Helikite (Allsopp Helikites Ltd, Hampshire, UK). A Helikite is an unique combination of a tethered balloon and a kite. Helikites are designed to be operated under extreme weather conditions. They fly stable even in strong winds and due to the kite wing additional lift is generated in windy conditions. For the measurements at the CVAO a 16 m³ Skyhook Helikite was used. The kite was attached to a 3 mm Dyneema rope (2000m long, ~ 4,6kg/1000m, Lyros D-Pro 3mm, breaking load 950 daN, working elongation < 1%) and operated by a winch (TROPOS built). Under calm conditions the Helikite has a net load capacity of ~ 8kg. At windy conditions the pull increases significantly and reaches about 16 kg at 6 m s^{-1}. Depending on the prevailing conditions, measurements up to an altitude of about 1000 m could be carried out. The payload with meteorological sensors was attached to rope about 20 m below the helikite. The payload here was a measuring system for standard meteorological parameters (p, T, rH, wind direction and velocity). The device is based on a microcontroller-based data logger (TROPOS). The sensors were digital sensors, tested and selected in the TROPOS wind tunnel (LACIS-T). Wind speed was measured using a differential pressure sensor together with a pitot tube, wind direction was determined from an orientation sensor (compass) of the wind vane. Data were recorded with a measuring frequency of 2 Hz, stored on SD card and additionally transmitted to a ground station (via XBee). In total 19 flights measured at 10 days are available.

Meteorological parameters and trace gases

Temperature, relative humidity and wind measurements were measured using a meteorological station fitted with various sensors (Campbell Scientific ltd, UK).

Ozone was measured using a UV absorption instrument (Model 49i Thermo Scientific).

VOCs and OVOCs were measured using a dual channel gas chromatograph with flame ionization detection (Agilent 7890-A). The instrument has two parallel columns, which simultaneously resolve C_2 - C_8 NMHCs and o-VOCS methanol and acetone using a more polar LOWOX column. VOCs are pre-concentrated onto a multi-adsorbent bed at -30 °C and then rapidly desorbed at 350 °C into helium flow using a desorption unit (Markes International Unity2). NMHCs are calibrated monthly using a multicomponent hydrocarbon standard (National Physics Laboratory, UK, typical concentrations ~ 5 ppbV) whilst for OVOCs a permeation system is used for calibration at levels of 8 to 25 ppbv in conjunction with relative detector response. Weighings of the OVOC permeation tubes are typically carried out every 6 weeks. The accuracy of the OVOC calibration is estimated as 10% for methanol and 5% for acetone. DMS was measured using a gas chromatograph with mass spectrometric detection (Agilent 7890-A, 5977 MSD). A Unity2 (Markes International) was used for the preconcentration of DMS onto a Tenax trap at -30° C which was desorbed at 350 °C into a flow of helium onto the GC. DMS was calibrated every ten hours during the campaign using a working standard manufactured at the University of York and quantified using relative detector response to benzene (10 ppm DMS standard, Korea Research Institute of Standards and Science, Republic of Korea (KRISS). All trace gas and meteorological measurements were made from a height of 17.5 m asl.

Plunging waterfall tank at the CVAO

The tank was designed to study the bubble driven transfer of organic material from the bulk water via the SML into the aerosol phase. It consisted of a 1400 L basin with a 500 L aerosol chamber on top. The basin (120 cm length x 110 cm width x 100 cm height) was made of 10 mm polyvinyl chloride (PVC) plates, held together by an aluminum frame. One side was transparent allowing for visual inspection. To minimize contamination from the tank walls, the entire basin was lined with a Teflon FEP bag. Inlet and sampling ports were made from Swagelok stainless steel fittings. PVC in contact with seawater was rinsed with artificial seawater for at least two weeks prior to use inside the basin. The head air space was made of Teflon FEP and had a total volume of 500 L (60 cm length, 110 cm width, 60 cm height). Sampling ports for bulk water and the SML were located on top of the basin. Bulk water samples were taken from 50 cm above the bottom and sampled into 1 L Duran glass bottles through a Teflon PFA tube using the hydrostatic pressure. Prior to each sampling, the tubing was first flushed with 100 mL of bulk water. SML samples were taken with a boron silicate glass plate (4 mm, 15 x 60 cm) via a slit in the enclosure. The SML sampling volume was limited to about 55 mL, corresponding to SML loss by about 50% when assuming SML layer thickness to be 60 to 80 µm (Falkowska 1999). The glass plate was cleaned with ultrapure water and ethanol prior to each sampling. Bubble driven transport of organic material was simulated using a skimmer on a plunging waterfall. The plunging waterfall (Fig. SI3) was made from a tubular pump (Osaga ORP 25000) that was placed at the bottom of the tank and a PVC tube of 100 cm length and 10 cm inner diameter. The tube towered 40 cm above the water surface. Water was pumped at a flow rate of approximately 200 L min^{-1} through the tube. The large diameter of the tubular pump and the tube ensured resulted in small pressure fluctuations and hence prevent the pelagic phytoplankton and microbial community from damage. The falling seawater simulated the process of wave breaking and was assumed to mimic the natural size spectra of rising air bubbles. A stainless steel inlet was inserted in the headspace of the tank and connected with three filter holders for offline aerosol particle sampling without size segregation (TSP). In addition, the stainless steel inlet was connected to a SMPS (same type as used for ambient aerosol particle characterisation) for online aerosol measurements. This method of aerosol generation resulted in a very efficient generation of nascent sea salt aerosols with aerosol particle size spectra centred around 100 nm as shown in Figure S2.

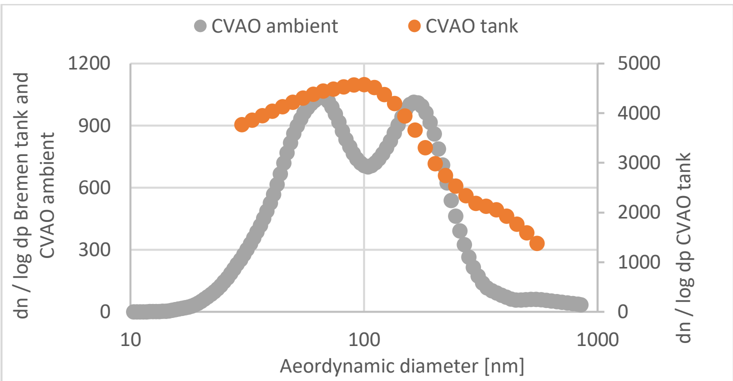

Fig. S2*: Size distribution of the aerosols generated in the tank experiments in comparison to the size distribution of ambient aerosols at the CVAO.*

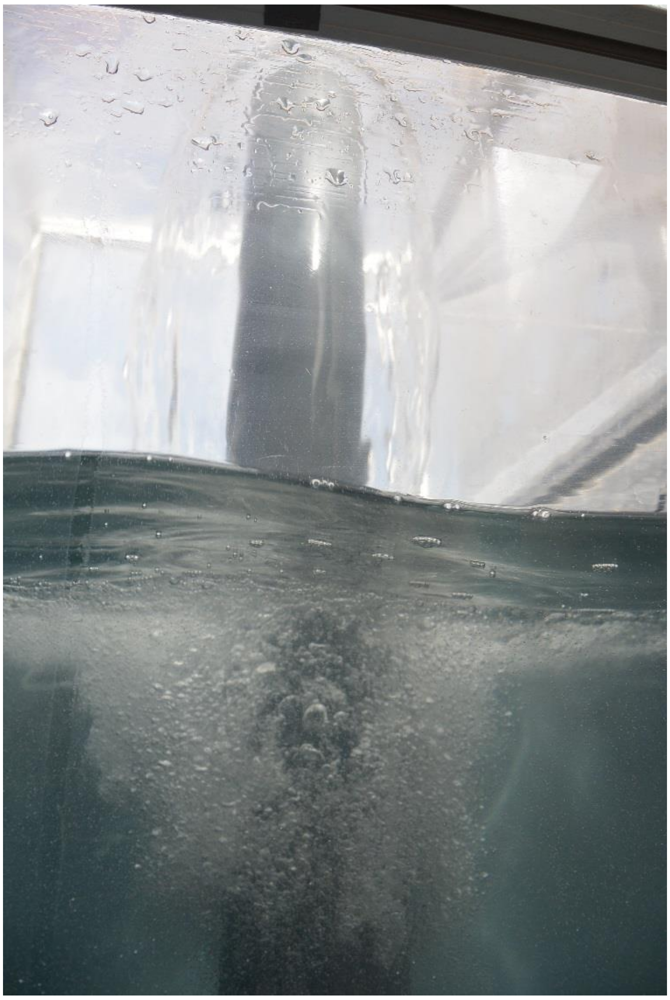

Fig. S3: *View of the plunging waterfall.*

The MarParCat

The MarParCat is a remotely controllable catamaran designed as a platform for water and SML sampling. It has a size of 245 x 180 x 140(l, w, h) and a total weight of 125 kg. The payload is approximately 160 kg. The catamaran is made from two Technus PE-floats (Type 90/150, 245 x 31 x 38 cm) hold together by an aluminum frame. The catamaran is powered with a 12V outboard motor (Minn Kota Traxxis 55) and uses two 12V 60 KwH lead batteries for power supply.

The SML is sampled by means of rotating glass plates (Duran, DWK Life Sciences, Germany). The glass plates have a diameter of 60cm and are placed 10 cm above the water surface in the gravity center of the catamaran. The plates rotated at a speed of 8 rpm. Depending of the thickness of the SML the sampling volume typically varied between 80 and 120 ml min^{-1} allowing to sample about 10 L SML within 2 h. The water collected in the wiper was transferred into 2x 5 L Duran glass bottles with a peristaltic pump (Verder M25, 12V. Prior sampling the SML sampling device was flushed for at least 15 minutes at the sampling site. Bulk water samples were collected at a rate of 120 ml min^{-1} from a depth of 70 cm using a peristaltic pump (Verder M25, 12V) and collected in two 5 L Duran glass bottles. The material of the tubing is Teflon PFA.

During the campaign, the catamaran was toweled to the sampling site with a fishing boat and typically operated 20 m apart from the fishing boat where manual SML sampling took place.

Aerosol particle sampling and chemical analysis of inorganic ions, OC/EC and WSOC

Aerosol particles (PM_1 and PM_{10}) were collected on preheated 150 mm quartz fiber filters (Minktell, MK 360) at a flow rate of 700 L min^{-1}. Size-resolved aerosol particles were sampled on pre-combusted aluminium rings with a Berner impactor. To avoid condensation of atmospheric water on the surface of the aluminium foils, a conditioning unit was mounted between the impactor inlet and the sampling unit consisting of a 3 m tube. By heating the sampled air, high relative humidity of the ambient air was reduced to 75-80% before the collection of the aerosol particles. The temperature difference between the ambient air at the impactor inlet and the sampled air after the conditioning unit was below 9 K. Sampling time was typically 24 h. After sampling, filters and aluminium foils were stored in aluminum boxes at -20 °C and transported in dry ice to the TROPOS laboratories in Leipzig, Germany. The chemical analysis of inorganic ions, the water soluble organic carbon (in the aerosol particles as well as in the ocean water and cloud water) and elemental carbon are described in detail in (van Pinxteren, et al. 2017; van Pinxteren, et al. 2015) and in Triesch, et al. (2019).

Ice nucleating particles: sampling and analysis

The quartz fiber filters mentioned in the previous paragraph (PM10, PM1 at CVAO and Mt. Verde) were used for INP measurements. INP concentrations were also analysed for bulk seawater and SML seawater collected at the seawater station Bahia das Gatas and in cloud water collected during cloud events on the mountain top (Mt. Verde). All of the filter and water samples were stored at -20 ℃ at Cape Verde and cooled below -20 ℃ during transportationto TROPOS, where all samples were again stored at -20 ℃ until they were prepared for the measurements. Two droplet freezing devices called LINA (Leipzig Ice Nucleation Array) and INDA (Ice Nucleation Droplet Array) (Chen, et al. 2018; Hartmann, et al. 2019) were deployed to characterize INP number concentrations (N_{INP}) from filter samples and in bulk and SML seawater, and cloud water, yielding results in the temperature range from roughly -5°C to -25°C.

SAS analysis

Phase sensitive alternating current (AC) voltammetry was applied for SAS analysis, being already used as a successful tool for the determination of SAS in a plethora of environmental aquatic samples (Frka, et al. 2009; Frka, et al. 2012; Kroflič, et al. 2018). Measurements (out-of-phase mode, frequency 77 Hz, and amplitude 10 mV) were performed with μAutolab-type II (Eco Chemie B. V., The Netherlands), GPES 4.6 software (Eco Chemie B. V., The Netherlands), followed the method of Ćosović and Vojvodić (1998). A standard polarographic Metrohm cell of 50 cm^3 with a three-electrode system was used: working electrode - hanging mercury drop electrode (HMDE; Metrohm, Switzerland; A = 0.01245 cm^2), reference electrode - Ag/AgCl/3 mol L^{-1} KCl, auxiliary electrode - platinum coil. Before each measurement, previously purified (450 °C for 5 h; charcoal organic residue removal) saturated NaCl (Kemika, Croatia) solution was added to the sample to adjust the electrolyte concentration to 0.55 mol L^{-1}.

Lipid analysis: seawater

Total lipid and lipid class quantitation was performed by Iatroscan thin layer chromatography–flame ionization detection (TLC–FID) (Iatroscan MK-VI, Iatron, Japan). Lipids were separated on Chromarods-SIII and quantified by an external calibration with a standard lipid mixture. Quantified lipid classes include hydrocarbons (HC), lipid degradation indices (DI) (fatty acid methyl esters (ME), free fatty acids (FFA), alcohols (ALC), 1,3-diacylglycerols (1,3DG), 1,2-diacylglycerols (1,2DG) and monoacylglycerols (MG)), wax esters (WE), phytoplankton energy reserves (triacylglycerols (TG)), membrane lipids including three phospholipids (PL) (phosphatidylglycerols (PG), phosphatidylethanolamines (PE) and phosphatidylcholines (PC)), glycolipids (GL) (sulfoquinovosyldiacylglycerols (SQDG), monogalactosyldiacylglycerols (MGDG) and digalactosyldiacylglycerols (DGDG)), sterols (ST) and pigments (PIG). Lipids indicating OM degradation (DegLip) comprise the sum of ME, FFA, ALC, DG, MG. The standard deviation accounted for 3 to 11% of the signal magnitude of lipid classes (Gašparović, et al. 2015; Gašparović, et al. 2017).

Lipid biomarker and isotope analysis: aerosol particles

Typically one half of the filter was used for the lipid analysis. The lipids were extracted with a 3:1 DCM mixture (4 times 40 ml) and the combined extracts were evaporated to a volume of 1 ml. The concentrated extract was dried with NaSO4 and subsequently saponified with KOH/MeOH (50 g L^{-1}, 1h, 80°C) and then evaporated to dryness. Afterwards the extract was fractionated over an aminopropyl-column into four fractions of different polarity following standard geochemical procedures (Hinrichs, et al. 2000). The fatty acids were converted to their respective methylester using a BF_3/MeOH reagent and the alcohols were sylilated with BSTFA in the presence of pyridine. Each fraction was dried under nitrogen and picked up in a small amount of hexane for the following analysis. Quantification was carried out with GC-FID and GC-MS was used for identification. Compound specific carbon isotope analysis was done by GC-C-IRMS.

Trace metal analysis

Size resolved aerosol particles were collected on polycarbonate foils (Wicom, Heppenheim, Germany) using a low-pressure Berner impactor with a PM10 isokinetic inlet at a flow rate of 75 l min^{-1}. The collected particles were impacted on the foils creating spots of compressed particles. The impacted spots were analyzed for their trace metal content using a **T**otal Reflection **X**-**R**ay **F**luorescence (TXRF) S2 PICOFOX (Bruker AXS, Berlin, Germany) spectrometer equipped with a Molybdenum X-ray source. Trace metals including Fe, Mn, Ca, Cu, Zn, Se, V, Cr, Pb, Ni, Ti, Rb, Sr, Ba, La, and Ce were analyzed with a detection limit of a few picograms. The sample preparation procedure and instrument specifications are described in detailed in Fomba, et al. (2013). Trace metals were used to identify days of mineral dust influence and its estimation.

Pigments and Chlorophyll-*a*

For pigment analysis, several liters of bulk water were collected in a water depth of approximately 30 cm by filling 5 L polypropylene bottles. The bulk water was filtered over GF-F filters (Whatman, Germany) and the filters were immediately frozen at -20 °C until analysis. For analysis, the GF-F filters were extracted in 5 mL ethanol, and 20 µL of the extract were injected into the HPLC (Dionex, Sunnyvale, CA, USA) under gradient elution using methanol/acetonitrile/water systems as eluents. Chlorophyll a, chlorophyll b, phaeophorbide a, phaeophorbide b as well as chlorophyllide a were detected with fluorescence detection (FLD) as described in van Pinxteren, et al. (2017). All other pigments were analyzed with a diode array detector (DAD. Standard components were used for peak assignment and external calibration.

DOM classes

SML, bulk and cloud samples and aqueous aerosol extracts for DOM classes were filtered through 0.45 µm Polyethersulfone (PES) syringe filters and stored chilled (0 to 4 °C) in pre-combusted glass "TOC" vials until analysis, which occurred within 2 days of sample preparation. LC-OCD-OND (Liquid chromatography with organic carbon detection and organic nitrogen detection), allows ~1ml of whole water to be injected onto a size exclusion column (SEC; 2 ml min^{-1}; HW50S, Tosoh, Japan) with a phosphate buffer (potassium dihydrogen phosphate 1.2 g L^{-1} plus 2 g L^{-1} di-sodium hydrogen phosphate x 2 H_2O, pH 6.58) and separated into five "compound-group specific" DOM fractions. The resulting fractions are identified using unique detectors for organic carbon, UV-amenable carbon and organic nitrogen Huber, et al. (2011). All peaks were identified and quantified with bespoke software (Labview, 2013) normalized to International Humic Substances Society humic and fulvic acid standards, potassium hydrogenphthalate and potassium nitrate. Cloud water and aerosol samples were blank corrected based on sample blanks that were extracted in the same way. No sample blanks were available for SML and bulk water samples.

TEP

Water samples (SML, cloud and bulk water) are then filtered onto 0.2um polycarbonate filters at low pressure and stained with alcian blue. We used the spectrophotometric method to analyse the stain (Passow and Alldredge 1995) which gives TEP in µg of xanthum gum equivalent (µgXeqL^{-1}).

Microbial cell counts

Prokaryotic cell numbers were counted via flow cytometry after water samples were fixed, flash-frozen in liquid nitrogen, and stored at -20°C. Prior measurements, all samples were stained with SYBR Green solution. Counting was performed after addition of latex beads serving as an internal standard. Further details can be found in Robinson, et al. (2019).
Small autotrophic cells were counted after addition of red fluorescent latex beads (Polysciences, Eppelheim, Germany) and were detected by their signature in a plot of red (FL3) vs. orange (FL2) fluorescence, and red fluorescence vs. side scatter (SSC). This approach allows discrimination between different groups of prokaryotic and eukaryotic autotrophs (Marie, et al. 2010) which in our case were size classes defined as *Synechococcus*-like cells and Nanoeukaryotes.

Nitrous acid (HONO) using a LOng Path Absorption Photometer (LOPAP)

Nitrous acid (HONO) was continuously measured using a commercialized LOPAP HONO analyzer (LOng Path Absorption Photometer, QUMA Elektronik & Analytik GmbH), which has been described in more details elsewhere. The instrument was placed in a ventilated aluminum box. The temperature of the stripping coil was held at 25°C using a thermostat.

HONO was collected into a stripping coil and immediately converted in azodye. HONO concentration is indirectly measured through the azodye absorption from 550 to 610 nm into long path optical cell (2 meters). Temporal resolution of HONO was fixed to 30 seconds. Sampling flow of the gas was 1 L min^{-1} . The uncertainty of HONO concentration was 10% (2σ) with a detection limit of few ppt under our measurement condition. HONO concentration was calibrated using a standard solution of NO_2^- (Titritisol Nitrite standard, 1000 mg L^{-1} NO_2^- in water). The instrument was frequently calibrated over the measurement period. To account for zero drift, automatic zero air measurements were operated for 1 hour every 6.5 hours.

GO: PAM

The photochemical setup consisted of a Quartz cell (2 cm diameter and 5 cm length) half filled with SML samples collected the previous day and irradiated by means of a Xenon lamp. This reactor was flushed by a flow of air containing a large concentration of ozone (ppm levels), triggering O_3/OH reactions at the surface, but also in the bilk of the SML samples. The gaseous products of these reactions were then injected into the Go:PAM where aerosol production could take place.

Characterization of cloud events at the Mt. Verde

Cloud events were frequently observed at MT. Verde and characterized by relative humidity (RH) values of 100 %. In addition, cloud events were verified from the PNSD as described in Gong, et al. (2020).

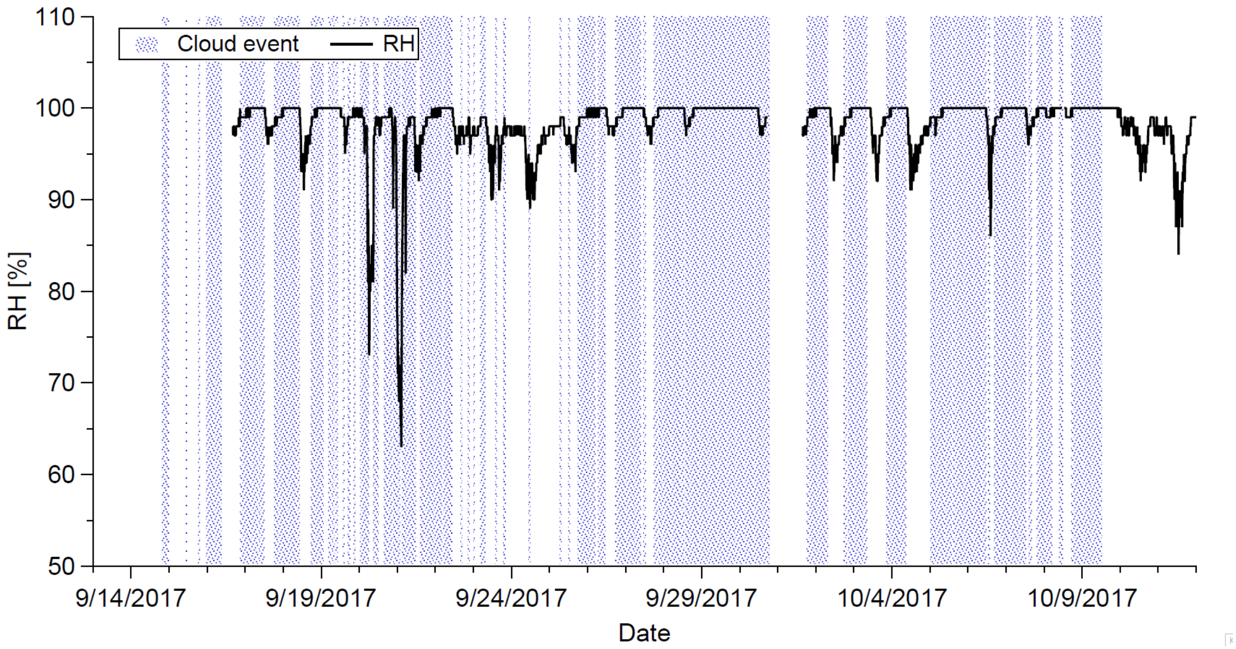

Fig. S4: *Time series of RH at Mt. Verde illustrated by the black line. Cloud event times are indicated by the blue shadows. The method and the figure are closely adopted from Gong, et al. 2020.*

Simulations I

The meteorological model data by COSMO are used to define a vertical meteorological data field as radio sounding data provided from the meteorological station Sal (Station number:

8594) are missing during the campaign. These data are used for meteorological 2D-simulations with COSMO-MUSCAT (Wolke, et al. 2012) that is done to calculate if a cloud will also occur over a flat surface area as from the 3D-simulations the effect of topography cannot be completely ruled out. Therefore, the meteorological model data by the Consortium for Small-scale Modeling-Multiscale Chemistry Aerosol Transport Model (COSMO), (Baldauf, et al. 2011) were used to define a vertical meteorological data field. For analyzing important multiphase chemical pathways, and the impact of the horizontal and vertical transport on the aerosol and cloud droplet composition within the MBL, the first model approach will be a box modeling study with the air parcel model SPACCIM (Spectral Aerosol Cloud Chemistry Model, Wolke, et al. 2005). SPACCIM is designed to investigate complex atmospheric multiphase chemistry processes. It has proven its excellent capability to investigate important multiphase chemical pathways (Hoffmann, et al. 2016; Hoffmann, et al. 2019; Tilgner and Herrmann 2010) Therefore, the simulations enable the determination of the most relevant multiphase chemical pathways for the chemical processing of marine aerosols during the campaign. The second model approach will apply 2D-simulations of the marine multiphase chemistry with the chemical transport model COSMO-MUSCAT (Baldauf, et al. 2011), which numerical scheme is able to treat cloud droplet chemistry (Schrödner, et al. 2014). Hence, the COSMO-MUSCAT simulations are able to investigate (i) the impact of horizontal and vertical transport on the chemical aerosol as well as cloud droplet composition and (ii) the direct and indirect impact of clouds on multiphase chemistry within, above and below the cloud. At the end of the simulations the model results will be compared with the measured aerosol concentration and composition and the in-cloud measurements at top of the Monte Verde mountain. For this purpose, a novel reduced marine multiphase chemistry module will be applied.

Simulations II

The simulations for the marine boundary layer height were carried out on three domains centred on Sao Vicente, Cape Verde, applying one-way offline nesting. The outer domain “N0” has a horizontal resolution of around 14 km and the two inner nests “N1” and “N2” have a grid spacing of 3.5 km and 0.875 km, respectively (see Fig. S5). The results shown in this work only refer to the inner nest “N2”.

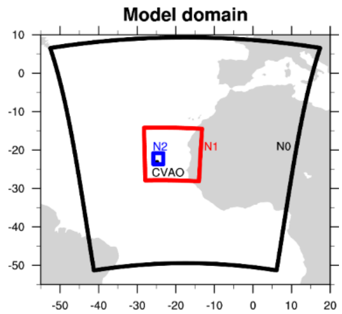

Fig. S5: *Model domains of COSMO-MUSCAT simulations performed within the MarParCloud project and geographical location of the Cape Verde Atmospheric Observatory (CVAO) at Sao Vicente, Cape Verde. Nested 14 km (black line), 3.5 km (red line), and 0.875 km (blue line).*

Table S1: Instruments employed at the CVAO during the campaign.

Measured parameter	Instrument	Performance	No. of measurements /samples (incl. blanks)	Running period	Responsible Institution
Chemical and biological composition of aerosol particles (PM_1. PM_{10}. TSP $_{h.v.}$. TSP $_{l.v.}$). INP measurements	Digitel sampler. 5-stage Berner impactor.High volume (h.v.) sampler. Low Volume (l.v.) samplers	8h to 48 h sampling	PM_1: 30 PM_{10}: 30 TSP $_{h.v.}$: 12 TSP $_{l.v.}$: 23 Impactor: 18x5 stages	15^{th} Sept – 11^{th} Oct	TROPOS. Leipzig, Germany
Physical characterization of aerosol size distribution	MPSS, APS, PNSD, CCNC	15 min sampling		13^{th} Sep – 13^{th} October	TROPOS. Leipzig
Meteorology	Automatic weather station	Minute samples		Continuous	NCAS. University of York. UK
VOCs, OVOCs,	Dual channel, gas chomatograph with flame ionization detection	Hourly samples		15^{th} Sep – 8^{th} October	NCAS. University of York. UK
Ozone	UV absorption	Minute samples		Continuous	NCAS. University of York. UK
Vertical profiles of meteorological parameters	Helikite	10 days of measurements	19 profiles	13^{th} Sep – 13^{th} October	TROPOS. Leipzig
SML and aerosol particles	Plunging waterfall tank	9 days of measurements	5 x SML and bulk water, 2 x 7 TSP samples	2^{nd} Oct – 10^{th} Oct	ZMT, Bremen, Germany
HONO	LoPAP	Continuously		15^{th} Sept – 11^{th} Oct	ICARE, Orleans, France
SOA forming potential	Go:PAM	Continuously for ambient air sampling	3 SML samples	15^{th} Sept – 11^{th} Oct	IRCELYON, Lyon, France.

Table S2: Instruments employed at the Mt. Verde during the campaign.

Measured parameter	Instrument	Performance	No. of measurements /samples (incl. blanks) during campaign	Running period	Responsible Institution
Chemical and biological composition of aerosol particles (PM_1. PM_{10}. TSP $_{h.v.}$. TSP $_{l.v.}$). INP measurements	Digitel sampler. 5-stage Berner impactor. Low Volume (l.v.) sampler	8h to 48 h sampling	PM_1: 19 PM_{10}: 19 TSP $_{l.v.}$: 3 Impactor: 7x5 stages	21th Sept – 09th Oct	TROPOS. Leipzig
Physical characterization of aerosol size distribution	MPSS, APS, PNSD, CCNC	15 min sampling		13th Sep – 13th October	TROPOS. Leipzig
Meteorology	Automatic weather station (Davis)	5 min sampling		Continuous	TROPOS. Leipzig
Cloud water for chemical. biological and INP measurements	Cloud water sampler (six samplers run in parallel)	2.5 – 13 h sampling	155	20th Sept – 09th Oct	TROPOS. Leipzig

Table S3: Details on bulk water and SML sampling at Bahia das Gatas at N16°53. W24°54.

Samp-ling date	Local sampling time (UTC-1)	Exact coordinates	Sampling device	Sampling conditions	Bulk water			SML			Sample ID
					salinity [ppt equals psU]	pH - value	temperature [°C]	salinity [ppt equals psU]	pH - value	temperature [°C]	
18.09.2017	11:35 -12:00	No data	GP*	very windy, big waves	34.1	8.1	25.0	-	-	-	Seawater 1
19.09.2017	8:38 -9:05	No data	GP	not reported	36.1	8.2	25.2	-	-	-	Seawater 2
20.09.2017	8:32 -9:54	N16°53.341 W24°54.360	GP	Slick and foam at the end of the sampling	36.3	8.1	26.7	36.2	8.1	26.7	Seawater 3
22.09.2017	8:56 -9:20	N16°53'48.002 W24°54'13.858	GP	very windy with big waves	-	-	-	-	-	-	Seawater 4
25.09.2017	9:45 -10:48	N16°53.753 W24°54.117	GP	calm sea	36.4	8.2	26.0	36.4	8.1	25.5	Seawater 5
26.09.2017	10:05-10:51	N16°53.934 W24.54.556	GP	not reported	36.3	8.2	25.1	36.1	8.1	26.4	Seawater 6
26.09.2017	11:10-11:50	N16°53.742 W24°54.061	CAT**	not reported	36.2	8.0	26.1	36.4	8.0	26.1	Seawater 6 (2)

27.09.2017	8:50 -10:03	N16°53.748 W24°54.134	GP	not reported	36.4	8.1	24.0	36.3	8.1	23.7	Seawater 7
27.09.2017	8:50 -10:03	N16°53.623 W24°54.257	CAT	not reported	36.2	7.9	27.0	36.0	7.9	26.7	Seawater 7 (2)
28.09.2017	9:15 -10:05	N16°53.623 W24°54.257	GP	not reported	36.5	8.1	27.8	36.6	8.1	26.8	Seawater 8
28.09.2017	9:15 -10:05	N16°53.623 W24°54.257	CAT	not reported	36.3	8.1	27.1	36.0	8.1	27.8	Seawater 8 (2)
02.10.2017	8:30 - 9:30	No data	GP	very windy, drift during sampling	36.0	8.2	20.9	36.5	8.3	20.9	Seawater 9
02.10.2017	8:30 -9:30	No data	GP	very windy, drift during sampling	35.9	8.2	22.7	36.1	8.1	23.9	Seawater 9 (2)
03.10.2017	8:15 - 9:35	N16°53.341 W24°54.360	GP	Not reported	36.1	8.2	22.8	36.6	8.2	21.0	Seawater 10
03.10.2017	8:15 - 9:35	N16°53.341 W24°54.360	CAT	not reported	36.2	8.2	23.5	36.3	8.2	22.4	Seawater 10 (2)
04.10.2017	8:15 - 9:00	N16°53'48.002 W24°54'13.858	GP	not reported	36.2	8.23	23.7	-	-	-	Seawater 11
04.10.2017	8:15 - 9:55	N16°53.934 W24.54.556	CAT	not reported	36.3	8.2	22.8	-	-	-	Seawater 11 (2)

05.10.2017	9:24 - 9:41	N16°53'44.824 W24°54'7.021	GP	smaller and higher waves in change	36.5	8.2	22.9	-	-	-	Seawater 12
06.10.2017	08:04-09:47	N16°53.753 W24°54.117	GP	windy	36.3	8.2	23.7	36.6	8.2	20.7	Seawater 13
07.10.2017	09:22 - 10:35	N16°53.742 W24°54.061	GP	very windy with long and short waves in change	36.4	8.2	21.8	36.7	8.2	21.2	Seawater 14
07.10.2017	9:17 - 10:46	N16°53.742 W24°54.061	GP CAT	very windy with long and short waves in change	36.5	8.2	22.4	36.7	8.2	24.5	Seawater 14 (2)
09.10.2017	8:30 - 9:17	N16°53.623 W24°54.257	GP	windy	36.4	8.1	23.6	36.6	8.2	21.5	Seawater 15
10.10.2017	8:30 - 9:30	N16°53.623 W24°54.257	GP	windy up to very windy with long waves	36.3	8.2	22.4	36.4	8.2	21.7	Seawater 16

**GP = glass plate, **cat = catamaran*

Table S4: Concentrations of pigments, DOC and microbial parameters in the SML and bulk water samples.

Sampling date		*18.09. 2017*	*19.09. 2017*	*20.09. 2017*	*22.09. 2017*	*25.09. 2017*	*26.09 .2017*	*27.09. 2017*	*28.09. 2017*	*02.10 .2017*	*03.10. 2017*	*04.10. 2017*	*05.10. 2017*	*06.10. 2017*	*07.10. 2017*	*09.10. 2017*	*10.10. 2017*
Sample ID		Sea-water 1	Sea-water 2	Sea-water 3	Sea-water 4	Sea-water 5	Sea-water 6	Sea -water 7	Sea-water 8	Sea-water 9	Sea-water 10	Sea-water 11	Sea-water 12	Sea-water 13	Sea-water 14	Sea-water 15	Sea-water 16
Parameter	unit																
pigments																	
chlorophyll c_2	µg L^{-1}	0.016	-	0.026	-	0.031	-	0.041	0.023	0.029	0.028	-	0.025	-	0.039	0.039	0.062
19 butanoyl oxyfucoxanthin	µg L^{-1}	0.000	-	0.017	-	0.002	-	0.018	0.004	0.019	0.012	-	0.013	-	0.026	0.031	0.058
19 hexanoyloxyfucoxanthin	µg L^{-1}	0.015	-	0.044	-	0.018	-	0.045	0.027	0.045	0.033	-	0.031	-	0.062	0.069	0.110
chlorophyll b	µg L^{-1}	0.021	-	0.042	-	0.055		0.038	0.032	0.050	0.061	-	0.035	-	0.063	0.065	0.109
chlorophyll a	µg L^{-1}	0.112		0.216	-	0.323	-	0.335	0.184	0.264	0.298	-	0.192	-	0.346	0.437	0.604
fucoxanthin	µg L^{-1}	0.014	-	0.044	-	0.093	-	0.171	0.040	0.045	0.060	-	0.037	-	0.105	0.153	0.223
phaeophorbide a	µg L^{-1}	0.031	-	0.032	-	0.047	-	0.041	0.037	0.034	0.036	-	0.033	-	0.037	0.039	0.038
phaeophytin a	µg L^{-1}	0.017	-	0.018	-	0.027	-	0.023	0.023	0.026	0.029	-	0.020	-	0.025	0.026	0.027
chlorophyllide a	µg L^{-1}	0.000	-	0.010	-	0.010	-	0.010	0.000	0.000	0.010	-	0.000	-	0.010	0.010	0.000
violaxanthin	µg L^{-1}	0.000	-	0.003	-	0.005	-	0.003	0.003	0.004	0.006	-	0.003	-	0.005	0.006	0.007
diadinoxanthin	µg L^{-1}	0.009	-	0.018	-	0.016	-	0.021	0.014	0.017	0.017	-	0.013	-	0.023	0.030	0.034
lutein	µg L^{-1}	0.001	-	0.002	-	0.005	-		0.003	0.002	0.003	-	0.002	-	0.003	0.003	
chlorophyll c_3	µg L^{-1}	0.014	-	0.022	-	0.027	-	0.038	0.017	0.025	0.025	-	0.022	-	0.035	0.034	0.059
peridinin	µg L^{-1}	0.003	-	0.005	-	0.007	-	0.006	0.003	0.007	0.005	-	0.006	-	0.005	0.005	0.008
zeaxanthin	µg L^{-1}	0.108	-	0.106	-	0.134	-	0.089	0.136	0.141	0.206	-	0.165	-	0.185	0.148	0.129
ß-carotine	µg L^{-1}	0.006	-	0.009	-	0.017	-	0.011	0.010	0.013	0.018	-	0.010	-	0.014	0.015	0.015
DOC																	
DOC SML (GP*)	µg L^{-1}	3260	2240	2780	2580	1680	2390	2020	2270	2020	2190	2050	-	3330	1610	1940	1820
DOC SML (cat**)	µg L^{-1}	-	-	-	-	-	2040	1450	1940	1520	1520	-	-	-	1850	-	-
DOC bulk water (GP)	µg L^{-1}	2800	1480	1090	1419	2370	1640	1070	1370	1340	1370	1090	1140	1290	947	1160	1290

DOC bulk water (cat)	µg L^{-1}	-	-	-	-	-	1810	1160	1280	1260	1260	1840	-	-	1480	-	-
microbial parameters																	
LNA (SML)	cells mL^{-1}	-	-	1.06E+06	-	1.48E+06	9.34E+05	1.05E+06	1.20E+06	9.90E+05	1.30E+06	1.15E+06	-	1.06E+06	-	-	-
HNA (SML)	cells mL^{-1}	-	-	8.91E+04	-	1.62E+05	5.85E+04	1.03E+05	1.23E+05	1.40E+05	7.84E+04	7.04E+04	-	9.58E+04	-	-	-
TCN (SML)	cells mL^{-1}	-	-	1.15E+06	-	1.64E+06	9.92E+05	1.15E+06	1.33E+06	1.13E+06	1.38E+06	1.22E+06	-	1.16E+06	-	-	-
synechococcus (SML)	cells mL^{-1}	-	-	4.42E+04	-	6.70E+04	2.71E+04	2.63E+04	2.61E+04	3.41E+04	7.40E+04	4.53E+04	-	2.42E+04	-	-	-
nanoeucaryotes (SML)	cells mL^{-1}	-	-	6.76E+02	-	1.64E+02	5.16E+01	5.16E+01	5.16E+01	1.85E+02	1.02E+01	2.05E+01	-		-	-	-
LNA (bulk water)	cells mL^{-1}	-	-	9.70E+05	-	1.24E+06	1.06E+06	1.07E+06	1.05E+06	1.72E+06	1.32E+06	1.21E+06	1.24E+06	1.18E+06	-	-	-
HNA (bulk water)	cells mL^{-1}	-	-	7.19E+04	-	1.17E+05	7.49E+04	9.15E+04	8.66E+04	6.07E+05	1.44E+05	7.91E+04	9.31E+04	9.88E+04	-	-	-
TCN (bulk water)	cells mL^{-1}	-	-	1.04E+06	-	1.36E+06	1.13E+06	1.16E+06	1.14E+06	2.32E+06	1.46E+06	1.28E+06	1.34E+06	1.28E+06	-	-	-
synechococcus (bulk water)	cells mL^{-1}	-	-	2.45E+04	-	4.27E+04	2.05E+04	2.63E+04	1.99E+04	6.82E+04	5.31E+04	3.79E+04	2.96E+04	2.42E+04	-	-	-
nanoeucaryotes (bulk water)	cells mL^{-1}	-	-	5.16E+01	-	1.54E+02	6.18E+01	1.23E+02	1.03E+02	1.46E+03	1.74E+02	6.14E+01	6.18E+01	1.06E+01	-	-	-

**GP: glass plate; *cat: catamaran (MarParCat)*

TCN: total bacterial cell numbers

HNA: high nucleic acid containing cells

LNA : low nucleic acid containing cells
- : no measurements available

**LOD: limit of detection*

Table S5: Concentrations and standard deviations (ng m^{-3}) of size resolved aerosol particle constituents measured in parallel during parallel measurements between 2.10 and 9.10 obtained from the CVAO (mean value of 5 blocks) and the Mt.Verde (mean value of 6 blocks) station. Aerosol particles were sampled in five different size fractions with aerodynamic particle diameter D_P (50% cut-off) from: 0.05-0.14 µm (stage 1), 0.14-0.42 µm (stage 2), 0.42-1.2µm (stage 3), 1.2-3.5 µm (stage 4) and 3.5-10 µm (stage 5).

CVAO	Sodium	Chloride	MSA	Sulfate	Nitrate	Oxalate	Ammonium	Potassium	Magnesium	WSOM	EC
stage 1	<LOD*	<LOD*	0.5±0.4	28.0±12	<LOD*	<LOD*	12.5±4	<LOD*	<LOD*	9.4±21	6.3±0.9
stage 2	<LOD*	<LOD*	12.7±2	741.9±111	<LOD*	3.2±4	232±48	3.7±5	0.3±0.6	38.6±16	27.5±14
stage 3	148±27	50.1±47	6.6±07	472.2±26	13.7±15	0.9±1	23.3±10	11.4±6	16.0±5.3	49.1±3	14.0±10
stage 4	1430±375	2300±680	4.5±0.9	572±159	698±76	22.1±8	16.6±4	54.4±11	156±33	108±6	12.5±1
stage 5	1520±306	2820±697	0.9±0.3	503±123	536±59	2.8±4	17.6±5	56.9±14	181±42	91.5±13	3.1±4

Mt. Verde	Sodium	Chloride	MSA	Sulfate	Nitrate	Oxalate	Ammonium	Potassium	Magnesium	WSOM	EC
stage 1	<LOD*	<LOD*	0.2±0.4	7.4±8	<LOD*	<LOD*	1.4±4	<LOD*	<LOD*	15.8±18	1.8±2
stage 2	<LOD*	<LOD*	2.1±1	111±54	<LOD*	0.3±0.4	36.5±22	0.3±0.7	<LOD*	26.9±21	15.0±12
stage 3	24.9±22	<LOD*	3.7±1	254±86	<LOD*	0.4±0.7	51.8±20	1.3±2.1	1.5±2.6	44.6±29	21.4±11
stage 4	163±110	277±171	2.3±0.7	156±62	96.5±68	0.3±0.8	12.6±10	2.9±5.1	13.4±8.5	80.2±29	3.6±5
stage 5	143±85	256±143	2.1±1	109±35	79.3±46	<LOD*	6.9±7	2.6±4.4	9.2±11	137±56	21.0±16

**LOD: limit of detection*

Table S6: Average concentrations and standard deviations of DOM fractions in the SML, bulk water and cloud water (ng L^{-1}) and in aerosol particles (PM_{10}) sampled at the CVAO and at the Mt. Verde (ng m^{-3}) sampled in parallel within the periods: 26. – 27.09., 01. – 02.10., and 08. – 09.10.2017.

	N	Biopolymers	Humic Substances	Building Blocks	LMW Neutrals	LMW Acids
SML	3	77±27	205±11	163±21	359±84	38±31
Bulk water	3	67±19	234±44	137±40	362±127	2±3
aerosol particles at CVAO	3	<LOD*	<LOD*	114±25	84±38	2±3
aerosol particles at Mt. Verde	2	<LOD*	<LOD*	55±23	58±22	6±4
Cloud water	4	27±21	354±222	242±224	301±227	58±98

**LOD: limit of detection*

References:

Baldauf, M., Seifert, A., Forstner, J., Majewski, D., Raschendorfer, M., and Reinhardt, T.: Operational Convective-Scale Numerical Weather Prediction with the COSMO Model: Description and Sensitivities, Monthly Weather Review, 139, 3887-3905, 10.1175/mwr-d-10-05013.1, 2011.

Chen, J., Wu, Z. J., Augustin-Bauditz, S., Grawe, S., Hartmann, M., Pei, X. Y., Liu, Z. R., Ji, D. S., and Wex, H. K.: Ice-nucleating particle concentrations unaffected by urban air pollution in Beijing, China, Atmospheric Chemistry and Physics, 18, 3523-3539, 10.5194/acp-18-3523-2018, 2018.

Ćosović, B., and Vojvodić, V.: Voltammetric analysis of surface active substances in natural seawater, Electroanalysis, 10, 429-434, 10.1002/(sici)1521-4109(199805)10:6<429::Aid-elan429>3.3.Co;2-z, 1998.

Falkowska, L.: Sea surface microlayer: a field evaluation of teflon plate, glass plate and screen sampling techniques. Part 2. Dissolved and suspended matter, Oceanologia, 41, 223-240, 1999.

Fomba, K. W., Müller, K., van Pinxteren, D., and Herrmann, H.: Aerosol size-resolved trace metal composition in remote northern tropical Atlantic marine environment: case study Cape Verde islands, Atmos. Chem. Phys., 13, 4801-4814, 10.5194/acp-13-4801-2013, 2013.

Frka, S., Kozarac, Z., and Ćosović, B.: Characterization and seasonal variations of surface active substances in the natural sea surface micro-layers of the coastal Middle Adriatic stations, Estuarine Coastal and Shelf Science, 85, 555-564, 10.1016/j.ecss.2009.09.023, 2009.

Frka, S., Pogorzelski, S., Kozarac, Z., and Ćosović, B.: Physicochemical Signatures of Natural Sea Films from Middle Adriatic Stations, Journal of Physical Chemistry A, 116, 6552-6559, 10.1021/jp212430a, 2012.

Gašparović, B., Kazazić, S. P., Cvitešić, A., Penezić, A., and Frka, S.: Improved separation and analysis of glycolipids by Iatroscan thin-layer chromatography-flame ionization detection, Journal of Chromatography A, 1409, 259-267, 10.1016/j.chroma.2015.07.047, 2015.

Gašparović, B., Kazazić, S. P., Cvitešić, A., Penezić, A., and Frka, S.: Improved separation and analysis of glycolipids by Iatroscan thin-layer chromatography-flame ionization detection (vol 1409, pg 259, 2015), Journal of Chromatography A, 1521, 168-169, 10.1016/j.chroma.2017.09.038, 2017.

Gong, X., Wex, H., Voigtländer, J., Fomba, K. W., Weinhold, K., van Pinxteren, M., Henning, S., Müller, T., Herrmann, H., and Stratmann, F.: Characterization of aerosol particles at Cabo Verde close to sea level and at the cloud level – Part 1: Particle number size distribution, cloud condensation nuclei and their origins , Atmos. Chem. Phys., 20, 1431–1449, https://doi.org/10.5194/acp-20-1431-2020, 2020.

Hartmann, M., Blunier, T., Brugger, S.O., Schmale, J., Schwikowski, M., Vogel, A., Wex, H., and Stratmann, F.: Variation of Ice Nucleating Particles in the European Arctic Over the Last Centuries, Geophysical Research Letters, 46: 4007-16, 2019.

Hinrichs, K. U., Summons, R. E., Orphan, V., Sylva, S. P., and Hayes, J. M.: Molecular and isotopic analysis of anaerobic methane-oxidizing communities in marine sediments, Organic Geochemistry, 31: 1685-701, 2000.

Hoffmann, E. H., Tilgner, A., Schrödner, R., Brauer, P., Wolke, R., and Herrmann, H.: An advanced modeling study on the impacts and atmospheric implications of multiphase dimethyl sulfide chemistry, Proc Natl Acad Sci USA, 113, 11776-11781, 10.1073/pnas.1606320113, 2016.

Hoffmann, E. H., Tilgner, A., Wolke, R., and Herrmann, H.: Enhanced chlorine and bromine atom activation by hydrolysis of halogen nitrates from marine aerosols at polluted coastal areas, Environmental Science & Technology, 53, 771-778, 10.1021/acs.est.8b05165, 2019.

Huber, S. A., Balz, A., Abert, M., and Pronk, W.: Characterisation of aquatic humic and non-humic matter with size-exclusion chromatography–organic carbon detection–organic nitrogen detection (LC-OCD-OND), Water research, 45, 879-885, 2011.

Kroflič, A., Frka, S., Simmel, M., Wex, H., and Grgić, I.: Size-Resolved Surface-Active Substances of Atmospheric Aerosol: Reconsideration of the Impact on Cloud Droplet Formation, Environmental Science & Technology, 52, 9179-9187, 10.1021/acs.est.8b02381, 2018.

Marie, D., Shi, X.L., Rigaut-Jalabert, F., and Vaulot, D.: Use of flow cytometric sorting to better assess the diversity of small photosynthetic eukaryotes in the English Channel, Fems Microbiology Ecology, 72: 165-78, 2010.

Passow, U., and Alldredge, A. L.: A dye-binding assay for the spectrophotometric measurement of transparent exopolymer particles (TEP), Limnology and Oceanography, 40, 1326-1335, 10.4319/lo.1995.40.7.1326, 1995.

Robinson, T.-B., Wurl, O., Bahlmann, E., Jürgens, K., and Stolle, C.:. 2019 b. 'Rising bubbles enhance the gelatinous nature of the air–sea interface', Limnology and Oceanography, 10.1002/lno.11188, 2019.

Schrödner, R., Tilgner, A., Wolke, R., and Herrmann, H.: Modeling the multiphase processing of an urban and a rural air mass with COSMO–MUSCAT, Urban Climate, 10, 720-731, 10.1016/j.uclim.2014.02.001, 2014.

Tilgner, A., and Herrmann, H.: Radical-driven carbonyl-to-acid conversion and acid degradation in tropospheric aqueous systems studied by CAPRAM, Atmos. Environ., 44, 5415-5422, 10.1016/j.atmosenv.2010.07.050, 2010.

Triesch, N., van Pinxteren, M., Engel, A., and Herrmann, H.: Concerted measurements of free amino acids at the Cape Verde Islands: High enrichments in submicron sea spray aerosol particles and cloud droplets, Atmos. Chem. Phys. Discuss., https://doi.org/10.5194/acp-2019-976, in review, 2020

van Pinxteren, D., Brueggemann, E., Gnauk, T., Mueller, K., Thiel, C., and Herrmann, H.: A GIS based approach to back trajectory analysis for the source apportionment of aerosol constituents and its first application, Journal of Atmospheric Chemistry, 67, 1-28, 10.1007/s10874-011-9199-9, 2010.

van Pinxteren, M., Fiedler, B., van Pinxteren, D., Iinuma, Y., Koertzinger, A., and Herrmann, H.: Chemical characterization of sub-micrometer aerosol particles in the tropical Atlantic Ocean: marine and biomass burning influences, Journal of Atmospheric Chemistry, 72, 105-125, 10.1007/s10874-015-9307-3, 2015.

van Pinxteren, M., Barthel, S., Fomba, K., Müller, K., von Tümpling, W., and Herrmann, H.: The influence of environmental drivers on the enrichment of organic carbon in the sea surface microlayer and in submicron aerosol particles – measurements from the Atlantic Ocean, Elem Sci Anth, 5, https://doi.org/10.1525/elementa.225, 2017.

Wolke, R., Sehili, A. M., Simmel, M., Knoth, O., Tilgner, A., and Herrmann, H.: SPACCIM: A parcel model with detailed microphysics and complex multiphase chemistry, Atmos. Environ., 39, 4375-4388, 10.1016/j.atmosenv.2005.02.038, 2005.

Wolke, R., Schroder, W., Schrodner, R., and Renner, E.: Influence of grid resolution and meteorological forcing on simulated European air quality: A sensitivity study with the modeling system COSMO-MUSCAT, Atmos. Environ., 53, 110-130, 10.1016/j.atmosenv.2012.02.085, 2012.